Synthesis of Membrane Permeable Macrocyclic Peptides Via Imidazopyridinium Grafting

Bo Li, Joshua Parker, Joel Tong, and Thomas Kodadek*

Abstract: Macrocyclic peptides (MPs) are a class of compounds that have been shown to be particularly well suited for engaging difficult protein targets. However, their utility is limited by their generally poor cell permeability and bioavailability. Here we report an efficient solid-phase synthesis of novel MPs by trapping a reversible intramolecular imine linkage with a 2-formyl- or 2-keto-pyridine to create an imidazopyridinium (IP^+)-linked ring. This chemistry is useful for the creation of macrocycles of different sizes and geometries, including head-to-side and side-to-side chain configurations. Many of the IP^+-linked MPs exhibit far better passive membrane permeability than expected for "beyond Rule of 5" molecules, in some cases exceeding that of much lower molecular weight, traditional drug molecules. We demonstrate that this chemistry is suitable for the creation of libraries of IP^+-linked MPs and show that these libraries can be mined for protein ligands.

Introduction

Macrocyclic peptides (MP) and related molecules have attracted considerable interest as probe molecules and drug leads, particularly for addressing difficult protein targets.[1] Macrocyclization of peptides imparts many favorable properties, including increased resistance to proteases, decreased conformational flexibility and, in certain special cases, increased cell permeability by promoting intramolecular hydrogen bonds that mask otherwise highly hydrated amide N-H moieties.[2] Moreover, powerful methods exist for the synthesis and screening of huge libraries of genetically-encoded MPs, such as phage display[3] and mRNA display[4]. Split and pool synthesis of DNA-encoded libraries (DELs) of macrocycles is another route to access large numbers of these molecules.[5] For such applications, there continues to be a need for new macrocyclization reactions that proceed with high efficiency under gentle reaction conditions, allow the introduction of novel functional groups, and suffers from little or no competitive intermolecular coupling.[6, 7] Here we report a new method for the macrocyclization of peptides that meets all of these criteria and confers on the products favorable pharmacological properties.

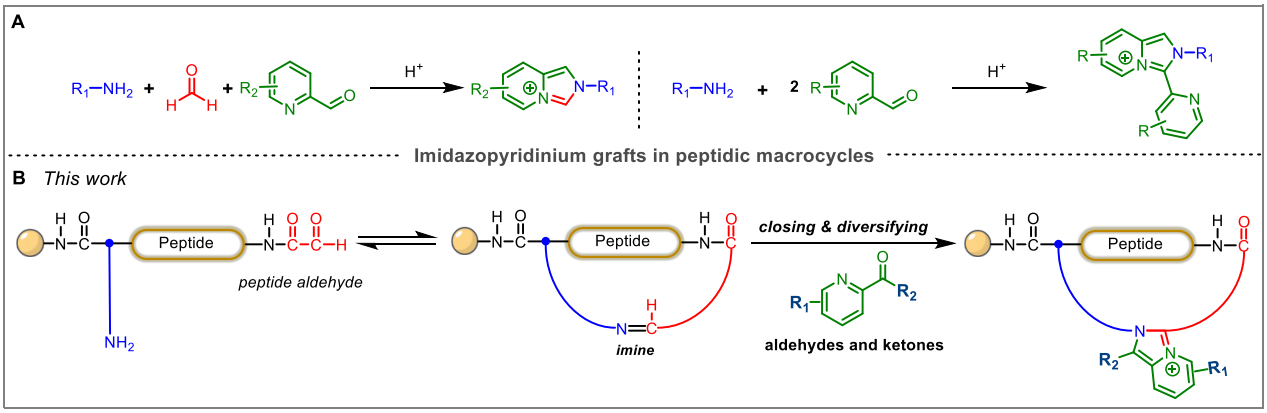

Scheme 1. Proposed solid-phase synthesis of MPs linked by an IP^+ ring. **A**. Established chemistry for the synthesis of the IP^+ moiety. **B**. Proposed application of IP^+ chemistry to the synthesis of MPs.

One common approach to the synthesis of MPs and other macrocyclic compounds is to trap an intramolecular imine linkage with an internal or external nucleophile.[7, 8] Depending on the imine trapping strategy, the products can range from simple amines to interesting heterocycles. Based on the work of Aron[9] and others,[10] we hypothesized that an alternative imine trapping strategy would be to expose the

imine to a 2-formyl- or 2-keto-pyridine to create a stable, imidazopyridinium (IP^+) unit (Scheme 1), a heterocycle that, to our knowledge, has not been incorporated into MPs previously. Given the broad availability of substituted pyridines, this would constitute a simple method to introduce additional diversity into MP libraries over and above that of the amino acids. Moreover, as explained below, we hoped that the IP^+ moiety would improve certain pharmacokinetic properties of MPs, particularly their passive membrane permeability.

In this study we demonstrate that cyclization via IP^+ formation is indeed a remarkably efficient and flexible method for the solid-phase synthesis of MPs. We also show that the reaction lends itself to the creation of bead-displayed libraries of IP^+-linked macrocycles and report the identification of a novel streptavidin ligand from such a library. Finally, we find that the IP^+ ring imbues these MPs with remarkably good passive membrane permeability, such that even molecules far beyond Lipinski's Rule of 5 (Ro5)[11] permeate membranes at rates comparable to low molecular weight, drug-like compounds.

Results

Solid-phase synthesis of IP^+-linked macrocycles. The IP^+ unit has been utilized in the synthesis of dyes[12] and compounds of pharmaceutical interest[13, 14, 15] However, the existing methods for synthesis of this heterocycle employ one equivalent each of formaldehyde, a primary amine and a pyridine-2-carboxaldehyde (P2CA) (Scheme 1A), or, alternatively two equivalents of P2CA and one equivalent of amine. These protocols cannot be utilized to create macrocycles using the approach shown in Scheme 1B.

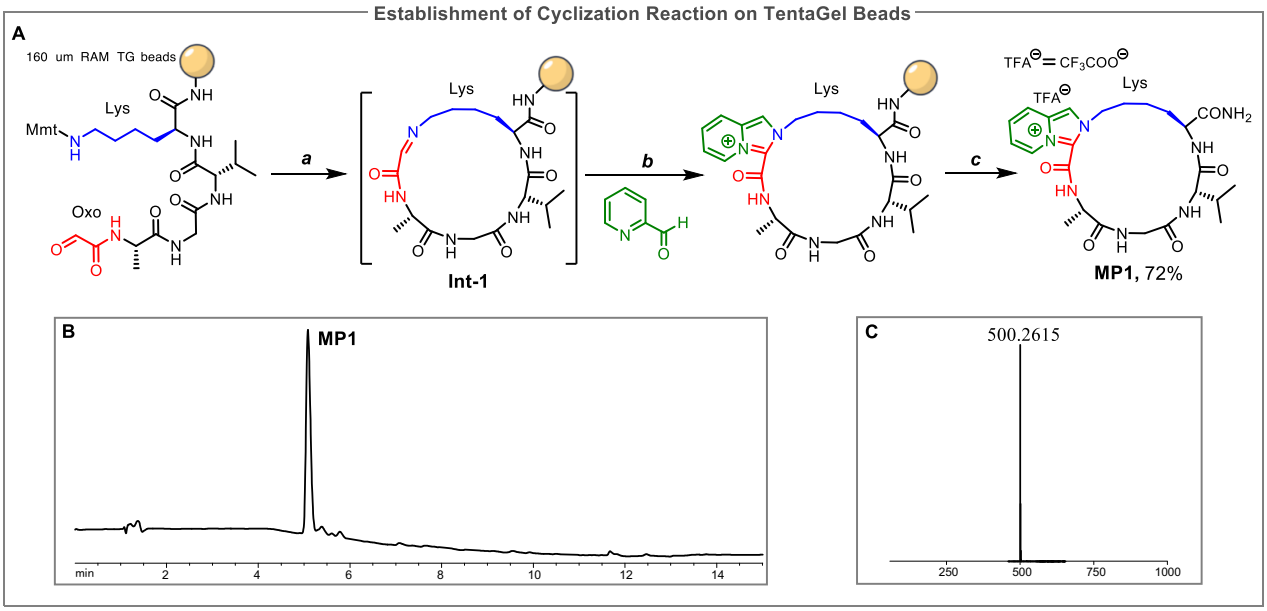

Figure 1. Solid-phase synthesis of an IP^+-linked MP **A:** The reaction was carried out on a 50 µmol scale based on loading. Mmt = Monomethoxytrityl. *a)* 25% HFIP/DCM, r.t., 2 x 30 min. *b)* AcOH/TFE (1:1, v/v), P2CA (3.0 equiv), rt., 10 hours. c*)* TFA, r.t., 40 min. **B:** Crude analytical HPLC trace of released cyclic peptide **MP1**. **C:** High-resolution mass spectrum of the crude material released from beads (**MP1**).

To explore the formation of macrocycles using this chemistry, we synthesized the model starting material shown in Figure 1A on 160 µm TentaGel beads with a Rink-amide (RAM) linker. Oxo represents the glyoxamide formed by $NaIO_4$-mediated oxidation of an N-terminal serine.[16] The Mmt protecting group was removed using a 1:3 mixture of hexafluoroisopropanol (HFIP)/DCM, then the beads were exposed to 3 equivalents of pyridine-2-carboxaldehyde in a 1:1 mixture of acetic acid (AcOH) /trifluoroethanol (TFE) for 10 hours at 30 °C. (While the reaction also could be carried out using 5% AcOH/TFE for 10

hours, 50% AcOH/TFE was found to reduce the “stickiness” of the beads to plastic microtiter plates and thus make the protocol more convenient). The products were released from the beads using trifluoroacetic acid (TFA) and analyzed by liquid chromatography/mass spectrometry (LC-MS). As shown in Figure 1, macrocycle **MP1** was formed in nearly quantitative yield. NMR analysis of the crude material (Supplementary Figure1) confirmed the high purity of the material as well as its structure. Indeed, when **MP1** was prepared on a large (50 µmol) scale, nearly pure compound was obtained in 72% yield by simply precipitating the material released from the bead with cold ether. No purification was necessary.

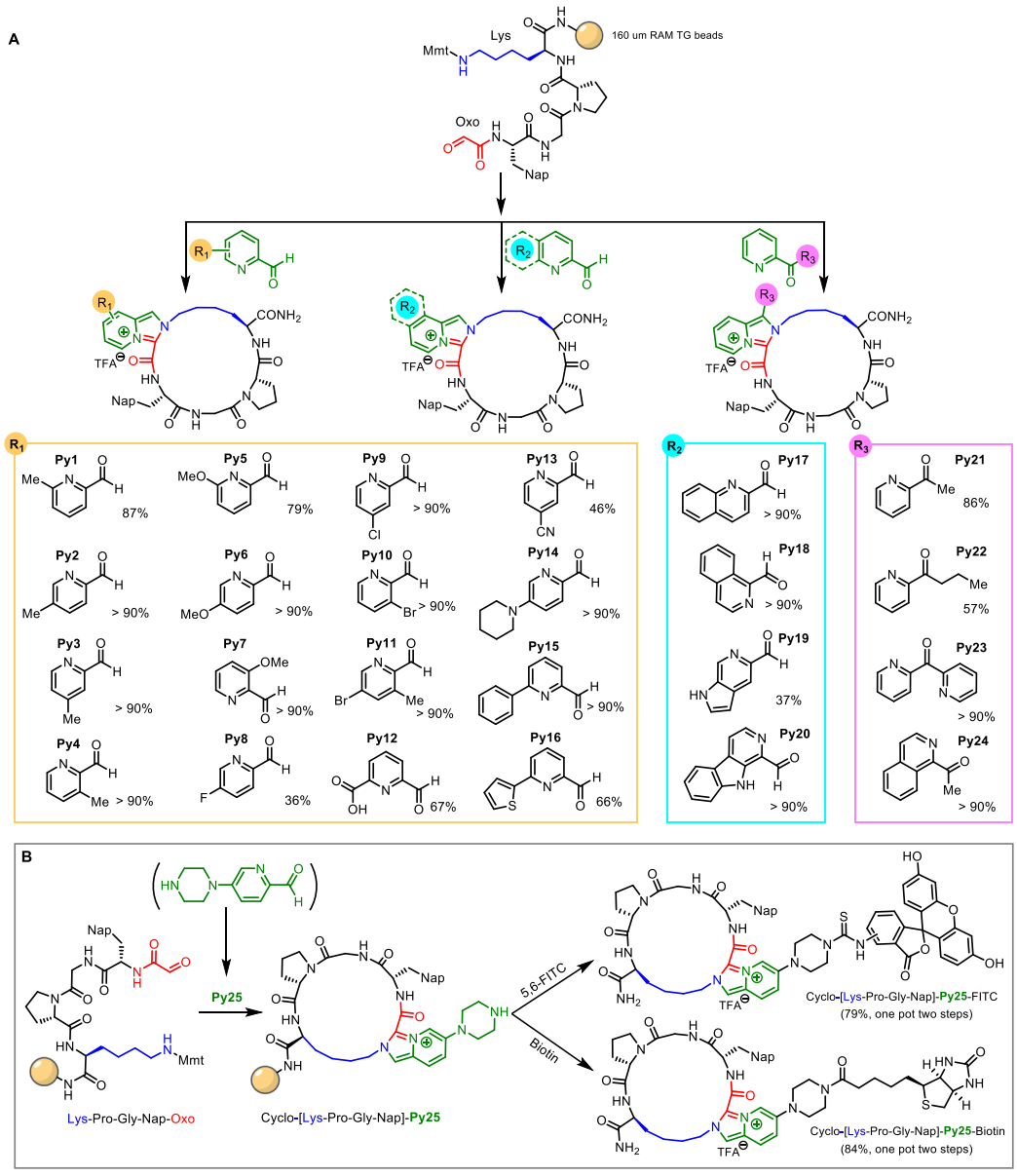

Figure 2. Various Aldehydes containing P2A motif for Macrocyclization. Aldehydes and ketones containing P2CA motif for cyclization. Nap (L-Ala(2-naphthyl)-OH) was used as UV indicator. All the reactions were carried out on a 2 µmol scale and the purity of crude product was determined by LC-MS. For the primary data see Supplementary Figures 5-29.

Given this promising result, we examined the scope of the reaction with respect to the P2CA unit. The results are shown in Figure 2. A wide variety of substituted P2CAs, carrying methyl, methoxy, chloro-,

bromo, piperidyl and phenyl groups, provide the IP^+-linked macrocycle in excellent yield and purity (>85%; **Py1-4, Py6-7, Py9-11, Py14-15**). P2CAs bearing electron-withdrawing groups such as -F, -CN or a carboxylic acid were less efficient substrates (**Py8, Py12, Py13**). We were also pleased to see that quinoline carboxaldehydes are also excellent substrates (**Py17, Py18, Py20**). Somewhat to our surprise, macrocyclization proceeded smoothly even with several 2-ketopyridines (**Py21-24**), further extending the number of substituents that can be introduced into the macrocycle using this strategy. We conclude that the scope of the reaction in the pyridine moiety is broad, though electron-withdrawing substituents result in somewhat lower yields.

Given the excellent result obtained with **Py14** and with an eye towards facile labeling of IP^+ MPs for future protein-binding studies, we synthesized **Py25** (Figure 2), with a piperazine group bearing a free secondary amine, and asked if this compound was a suitable substrate. Gratifyingly, macrocyclization proceeded efficiently (Supplementary Figure 30). The amine was readily modified with common labels such as biotin or carboxyfluorescein (Figure 2 and Supplementary Figures 31-32).

We next probed the scope of the reaction with respect to ring size. A series of linear precursors were synthesized in which 0-9 alanine residues separated the reactive Oxo and lysine (Lys) units (Figure 3A). Beads displaying these molecules were then subjected to the reaction conditions described above using 2-formyl-quinoline to close the macrocycle. After release from the beads the products were analyzed by LC-MS (see Supplementary Figures 33-39). Compound **MP2**, in which no spacer alanine was present, was produced in only about 5% LC yield. A single alanine spacer resulted in about half of the starting material being converted to the desired product. The linear peptides containing 2-5 alanine units provided a high yield of clean product. The yield decreased again using peptides containing 6-9 alanine residues. We conclude that this chemistry is optimally suited to provide MPs containing 15-24 atoms from canonical amino acids and can also yield useful amounts of MPs with 12 and 27-30 atoms in the ring.

We then turned to the synthesis of various MPs in this size range that contain a variety of residues. As shown in Figure 3B, various protected amino acids were compatible with this reaction using the standard conditions with various P2CAs (for polar amino acids, the protecting groups were removed after cyclization). Cyclization proceeded efficiently (see Supplementary Figures 40-45) with substrates containing Tyr (**MP12**), Trp (**MP13**), Arg (**MP13**), Lys (**MP14**), Cys (**MP15**), His (**MP16**), Glu (**MP17**). Methionine residues are oxidized quantitatively to the sulfoxide (see compound **MP14**) by $NaIO_4$, as expected.[17] The structures of these macrocycles were confirmed by LCMS and NMR spectroscopy (see Supplementary Figures 40-45).

We also revisited the synthesis of mixed residue MPs with ring sizes greater than 24 atoms. It is possible that the fall off in yield for substrates containing more than five consecutive alanine residues (Figure 3A) is due to a propensity to form helices that hinder cyclization. Therefore, we constructed linear peptides in which more flexible units (Ahx and Ipa) were placed between the reactive amine and Oxo residues. As seen in Figure 3B, this indeed resulted in efficient macrocyclization for compounds (**MP18** and **MP19**) with 37 and 39 atoms, respectively, in the ring (see Supplementary Figures 46-47). Based on these data, we speculate that the IP+ chemistry will be useful for the efficient synthesis of macrocycles spanning a much wider range of ring sizes than might have been suggested from the data shown in Figure 3A so long as there is sufficient flexibility in the linear precursor to allow formation of the intramolecular imine intermediate.

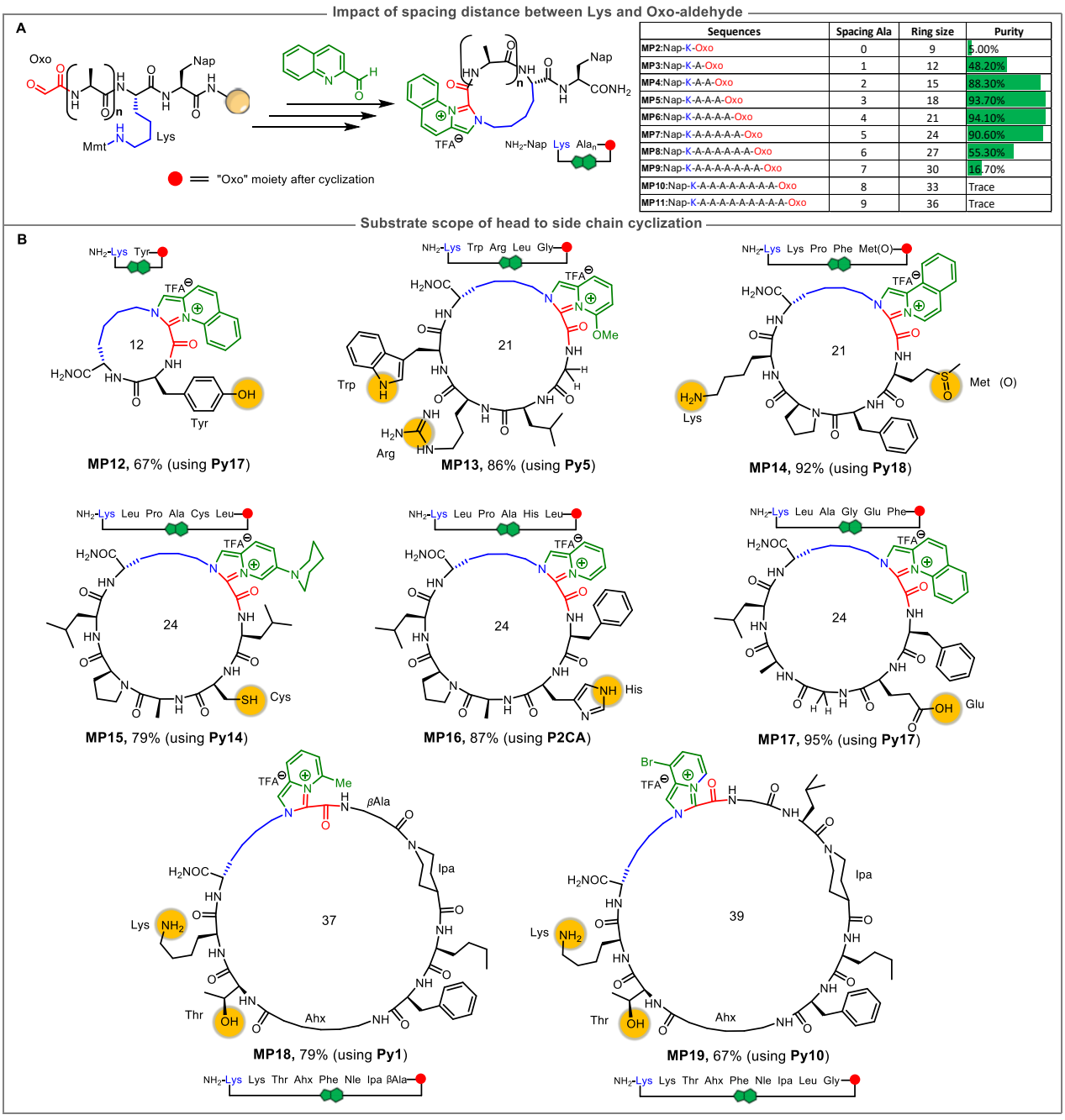

Figure 3. Side-to-head cyclization on TG Beads. A. Each linear peptide precursor was prepared on a 2 μmol scale on TG beads. Red balls represent the former glyoxamide unit after cyclization **B**. All the reactions were carried out on a 10 μmol scale based on loading. The purity of crude product was determined by HPLC and is shown in the figure. See supplementary information for details about isolated yields. Ahx: 6-aminohexanoic acid; Ipa: Isonipecotic acid.

We also examined the application of IP^+ chemistry to the synthesis of MPs in which the linkage is between an Oxo-modified side chain and an amine-containing side chain, such as a Lys or Dap residue (see Supplementary Figures 48-51 for the synthesis of these peptide precursors). As shown in Figure 4, side chain-to-side chain-connected MPs with different ring sizes were obtained in excellent purity using a variety of P2CAs.

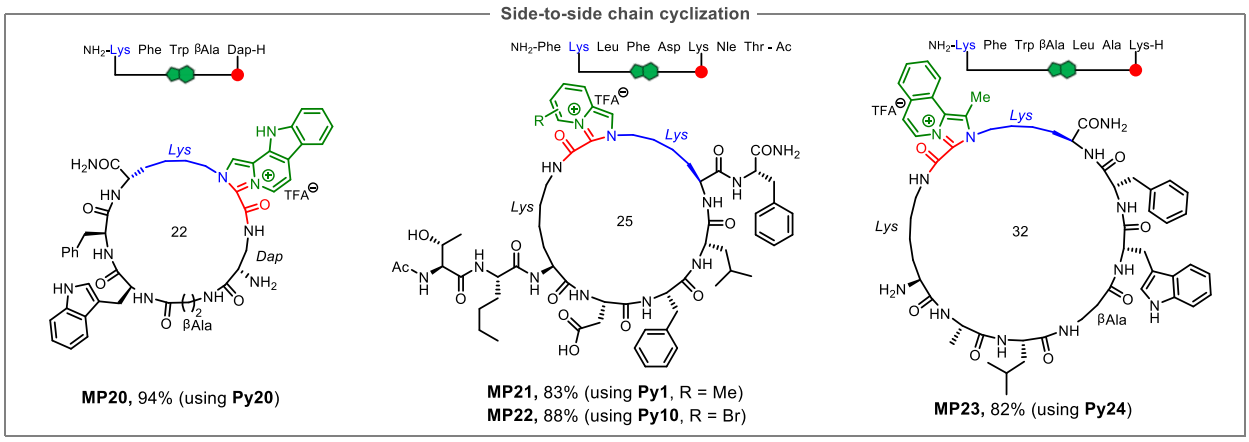

Figure 4. MP synthesized using side chain-to-side chain linkages. All the reactions were carried out at 10 μmol scale based on beads loading. Purity of crude product determined by HPLC was given. Dap: L-2,3-diaminopropionic acid; βAla: β-Alanine; Nle: L-norleucine. Red balls represent the glyoxamide-derived residues after cyclization.

Stapled peptides via IP$^+$ formation

Motivated by the broad success of the macrocyclization reactions presented above, including the side chain-to-side chain connections, we examined the utility of the IP$^+$-forming reaction for "peptide stapling" (Figure 5). This is a technique in which appropriately positioned side chain residues are linked covalently to stabilize an alpha-helical conformation of the peptide.[18] Stapled peptides are of broad interest as inhibitors of protein-protein interactions. For example, a stapled peptide inhibitor of p53-Mdm2/MdmX binding has recently entered clinical trials for the treatment of certain cancers with wild-type p53.

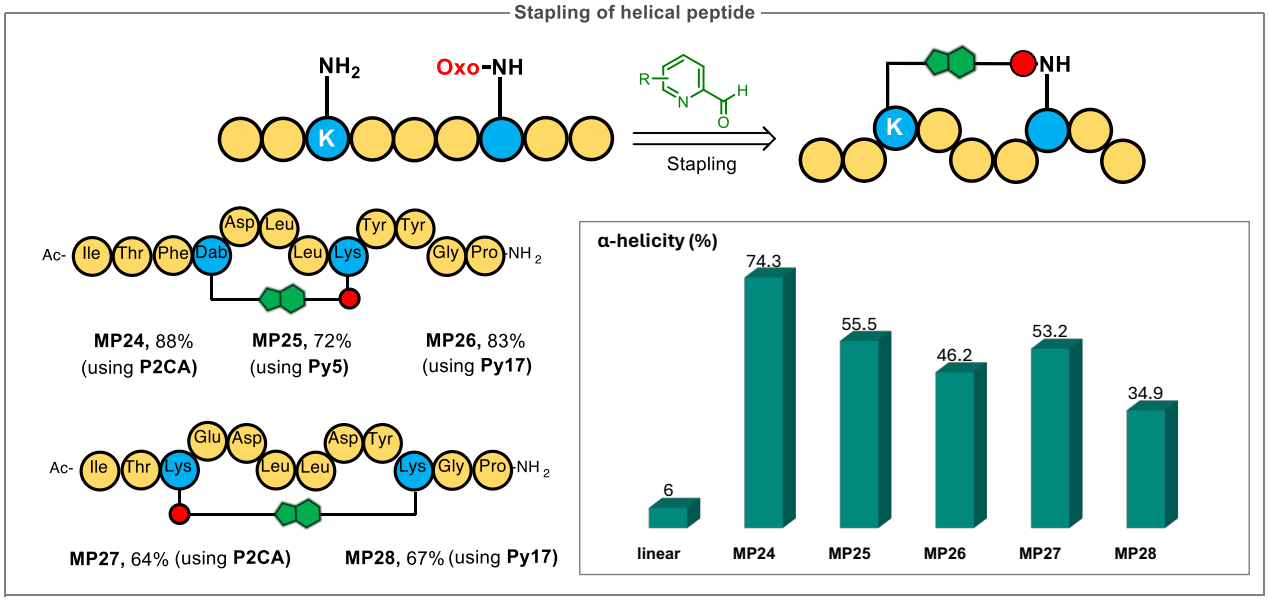

Figure 5. **Creation of stapled via IP$^+$ chemistry**. All the reactions were carried out at 10 μmol scale based on beads loading. Purity of crude product determined by HPLC was given. The spectra were obtained using 100 μM of the stapled peptide dissolved in 30% trifluoroethanol (TFE)/PBS (pH=7.4).

As a model we focused on the twelve amino acid peptide ITFEDLLDYYGP-NH_2 which is a ligand for the HIV capsid protein that disrupts capsid assembly in vitro, but not in cultured cells due its cell impermeability. Zhang, et al. used olefin metathesis chemistry to create a stapled version of this peptide (NYAD-1: IPFXDLLXYYGP; where X = a residue with an alkene-containing side chain) with much higher helical content than the native peptide and improved cell penetration properties. NYAD-1 is a modestly potent inhibitor of HIV replication in cultured cells.[19]

We constructed the five linear substrates shown schematically in Figure 4B in which the amino- and Oxo-containing residues had an i-i+4 or i-i+7 spacing. The beads displaying these compounds were treated with the indicated P2CA under the standard conditions. After cleavage the products were analyzed by LC-MS. In each case, good to excellent conversion to the desired stapled peptides was observed (see Supplementary Figures 52-56). The degree of helicity was determined by circular dichroism spectroscopy. As shown in Figure 5, the linear peptide was a random coil. All of the stapled MPs displayed an enhanced degree of helical content. The best of these (≈ 74% helical) was **MP24**, in which the i and i+4 residues had been stapled with **P2CA**. It is interesting that **MP24**, **25** and **26**, which contain the same ring but were formed using a different P2CA, display markedly different levels of helicity. The two i-i+7-stapled peptides (**MP27** and **MP28**), linked using **P2CA** and **Py17**, also displayed measurably different levels of helicity. These data suggest that the use of different P2CA units in the creation of IP^+-stapled MPs will provide a novel tool to fine tune the helical content of stapled peptides.

Parallel solid-phase synthesis of IP^+-linked MP libraries

Given the high level of efficiency and broad scope of the IP^+-forming macrocyclization reaction, we examined if this chemistry is suitable for the synthesis of MP libraries. Specifically, it was of interest to determine if the entire process could be miniaturized so as to be carried out on a small amount of TentaGel resin in the wells of a microtiter filter plate, which is the most convenient format for the creation of combinatorial libraries,[20] including DNA-encoded libraries (DELs).[21] To evaluate this issue, 20 different peptides, including eight tetrapeptides, four pentapeptides and four hexapeptides, were synthesized on 2 mg of 160 μm TentaGel RAM beads in individual wells of a 96 well microtiter filter plate open to the air. 18 of the 20 peptides had Mmt-protected Lys as the C-terminal residue, included a UV-active Nap, tyrosine (Tyr) or tryptophan (Trp) residue to facilitate subsequent LC-MS analysis, and terminated in a serine residue (subsequently oxidized to a glyoxamide). **L15 and L16** contained the protected Lys as the third residue. **L17** has a glyoxamide installed on a side chain. After completion of the peptide chain, the Lys and serine residues were deprotected and the peptide was oxidized with $NaIO_4$ to create the Oxo unit. Finally, three equivalents of a P2CA were added to each well to create the IP+-linked macrocycle. This protocol was carried out for five identical plates but in each case a different P2CA unit was added at the end. After incubation and washing, the material was released from the beads and completely deprotected using TFA. The products were analyzed by LC-MS.

Gratifyingly, the overwhelming majority of the products were produced in good to excellent purity (**Figure 6**). 83 of the IP^+-containing MPs were >85% pure and 13 were 75-85% pure. Only 4 of the 100 MPs were produced in < 75% purity (see Supplementary Figures 58-77 for the primary data). These data strongly support the idea that the IP+ grafting chemistry is suitable for the creation of libraries of MPs.

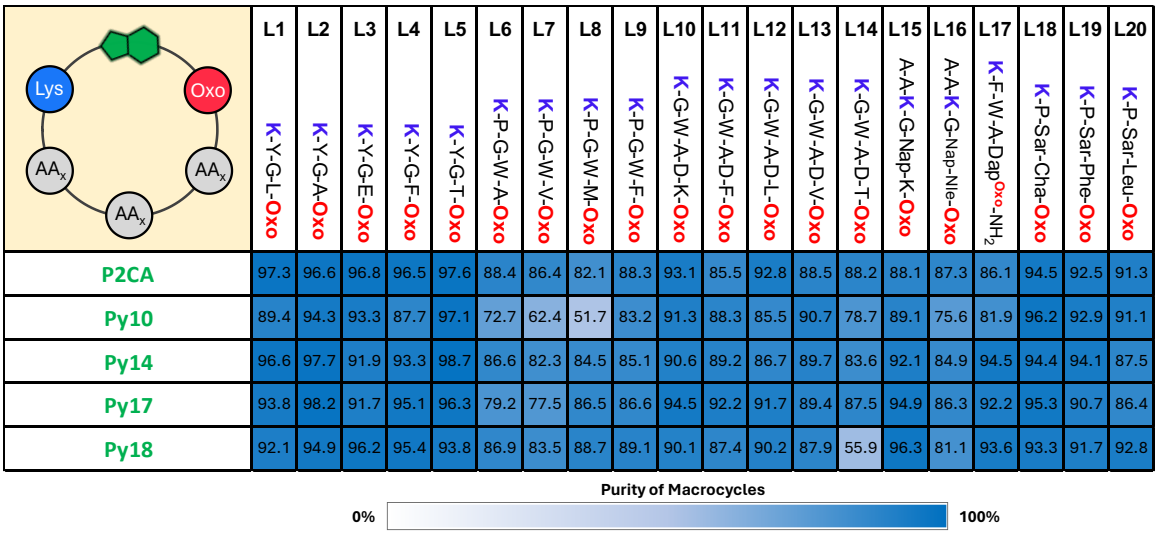

Figure 6. Solid-phase synthesis of 100 IP+-linked MPs in individual wells of a microtiter plate. The numbers indicate % conversion to product.

With this result in hand, we turned to the synthesis of a model screening library. The tripeptide sequence HP(Q/Y) has been shown to be a modest affinity ligand for Streptavidin (SA). To test the feasibility of making a small library of IP^+-linked MPs and screening it against a target protein, we constructed a library of 480 compounds on 10 µm TentaGel beads by parallel solid-phase synthesis in microtiter filter plates and tested each set of beads for their ability to capture fluorescently labeled SA. The general structure of the library is shown in **Figure 7**. A C-terminal Lys residue and an N-terminal Oxo unit flanked four variable positions in which one of 14 different amino acids was employed (Figure 7A). To bias the library towards peptides that resemble HP(Q/Y), amino acids **aa1, aa2, aa3**, and **aa11** were employed in the first position, amino acids **aa1-aa3** and **aa8-aa10** in the second position, amino acids amino acids **aa12-aa14** in the third position and amino acids **aa4-aa7** in the fourth position. The linear precursors were then treated with one of five different P2CAs (Figure 7A) to complete the synthesis.

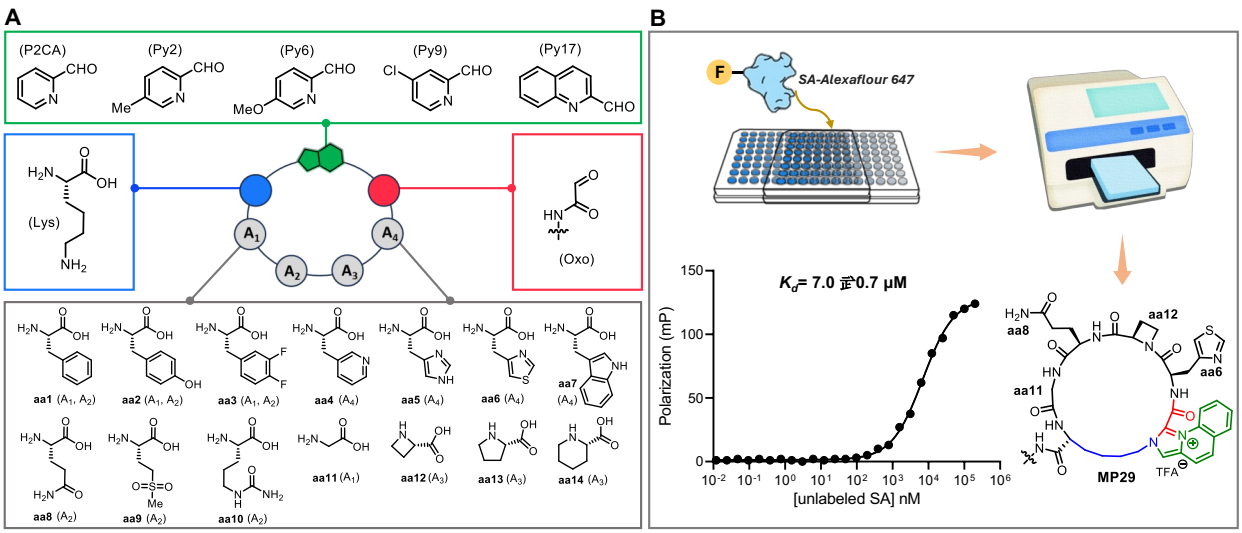

Figure 7. Synthesis and screening of an IP^+ MP library. **A**. General structure of the library and the building blocks used in its construction. The position(s) at which each amino acid building block was employed in construction of the library is indicated at the bottom of the figure (A1, A2, etc.) **B**. Top:

Schematic of the screening protocol used to identify ligands for fluorescently labeled Streptavidin (SA). Bottom: Increase in fluorescence polarization as a result titration of fluorescein-labeled **MP29** (structure shown on right without the fluorescein) with unlabeled SA. See text for details of the library construction and screening.

After thorough washing and equilibration in an aqueous buffer, the beads were blocked with Starting Block to discourage non-specific protein binding, then incubated for one hour with Alexaflour 647-labeled SA (A647-SA, 150 nM) at room temperature. After thorough washing, the amount of fluorescence retained by the beads in each well was measured using a fluorescent plate reader. This protocol was conducted in triplicate. The five bead-displayed MPs that retained the highest levels of A647-SA in each run were synthesized as C-terminal fluorescein conjugates and their solution affinities for unlabeled SA were determined by titration followed by an increase in fluorescence polarization (Figure 7B). These data showed IP^+-linked **MP29** to be the best SA ligand with a K_D of approximately 7.0 μM (Figure 7B). These data demonstrate that the IP^+ chemistry is suitable for the construction of useful screening libraries of novel MPs.

Evaluation of the passive membrane permeability of IP^+-linked MPs

As mentioned above, a major limitation of most MPs is that they display poor passive membrane permeability, limiting their utility for engaging intracellular targets. The IP^+ motif is an interesting functional unit with respect to potentially influencing membrane permeability. It is relatively hydrophobic, especially in the case where quinoline or other more highly substituted P2CAs are employed to create the macrocycle, yet it carries a permanent positive charge (i.e., not due to a protonation event). It seems reasonable to hypothesize that the positive charge might concentrate the compound on the cell surface through electrostatic interactions and that the hydrophobic character of the heterocycle might stimulate movement across the membrane, resulting in improved passive membrane permeability.

To evaluate this idea, we prepared twenty different IP+-linked MPs of various sizes and compositions and measured their rates of membrane transit using PAMPA (parallel artificial membrane permeability assay). Propranolol, a highly permeable low molecular weight (259 Da) drug and the much less permeable charged small molecule Ranitidine were employed as controls. In this assay compounds displaying a -log Pe below 6.0 are considered to be highly permeable, while those with a -log Pe between 6.0-7.0 are considered to be moderately permeable.

As shown in Figure 8A, a remarkable 45% of the MPs tested displayed a -logPe value below 6.0 (green dots), despite the fact that the masses of these compounds are all well above 500 Da (Figure 8B). One of these macrocycles (**MP40**), with a molecular weight of 846 Da, actually traversed the membrane more rapidly than Propranolol. The particular P2CA used to create the macrocycle clearly had a significant effect on permeability. For example, four MPs with the same peptide component, but formed using different P2CAs (second row of Figure 8B), displayed significantly different permeabilities, ranging from -logPe = 4.6 to 6.0.

We also tested the permeability of two very large compounds, **MP18** and **MP19** (see Figure 3B for structures), which have molecular weights of 1071 Da and 1234 Da, respectively. Remarkably, even these >1000 Da compounds displayed moderate membrane permeability in the PAMPA (-logPe of 6.4 and 6.3, respectively). Taken together, these data suggest that IP+-containing MPs display much better membrane permeability than typical peptide macrocycles.

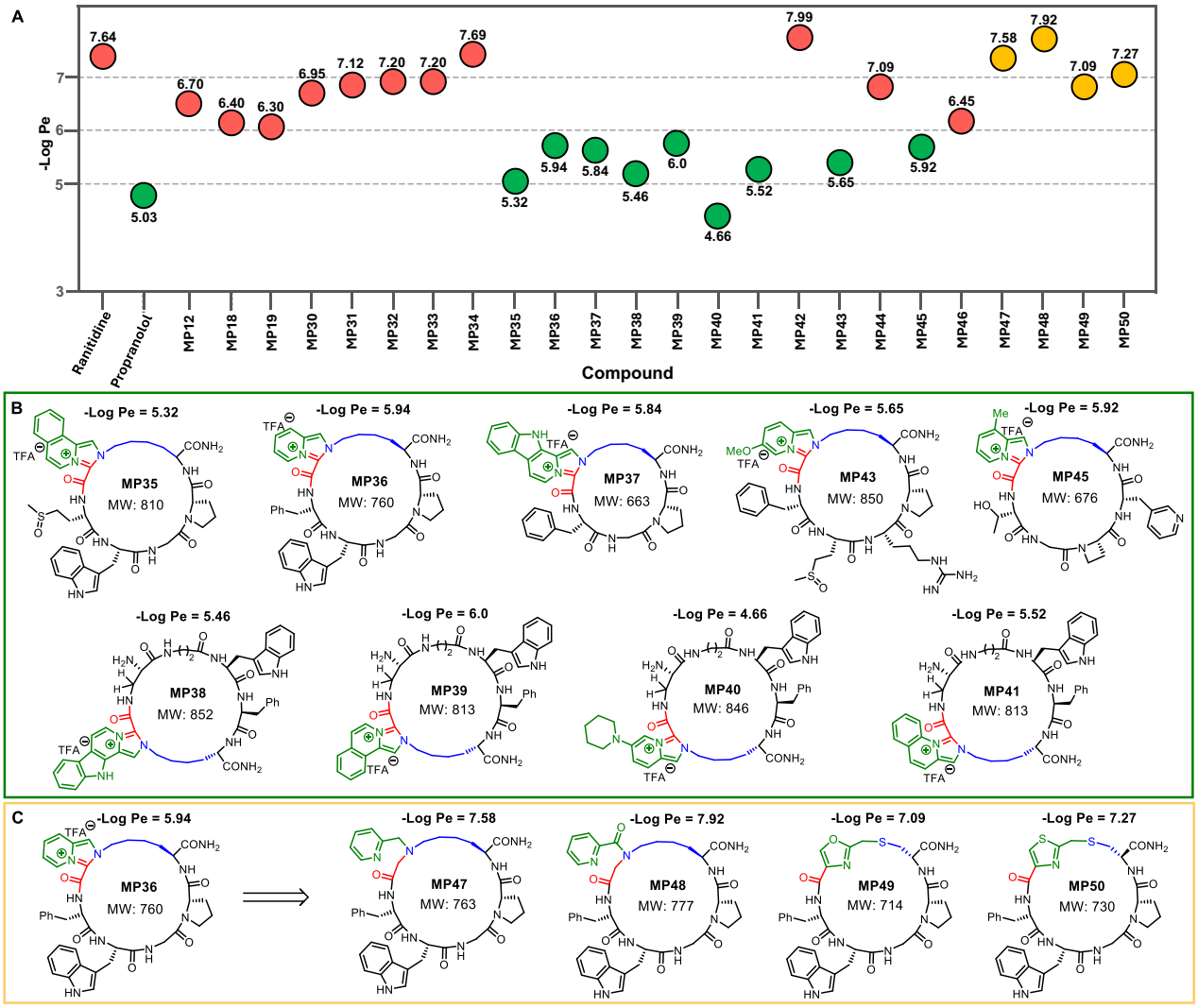

Figure 8. Passive membrane permeability of IP⁺ MPs. **A**. Rates of membrane passage (expressed in units of -logPe) for the compounds indicated as measured using PAMPA. **B**. Structures of the most permeable MPs (see Supplementary Figure 82 for a complete listing of the compounds analyzed). **C**. Structures of **MP36** analogues lacking the IP+ unit. Their (poorer) passive membrane permeability is shown in A (yellow dots).

To directly compare the permeability of an IP+ macrocycle with non-IP+ analogues, we chose **MP36** as a model. This compound displays a -logPe value (5.94) close to the median of the 20 MPs we analyzed. We then synthesized various analogues of MP36 (Figure 8C). **MP47** and **MP48** were created using intramolecular amination or acylation chemistry to close the ring. This is the equivalent of opening the pyridinium ring and deleting the positive charge. **MP49** and **MP50** were created by closing the ring through thioether bond formation and thus lack any trace of the IP⁺ moiety. The passive permeabilities of these four molecules were assessed using PAMPA. As shown in Figure 8A (yellow dots), each of these molecules displayed a passive permeability between 10- and 100-fold poorer than the IP⁺-containing **MP36**. This comparative assessment shows that the IP⁺ unit has a major positive effect on the passive membrane permeability of the MPs.

Entry of IP$^+$ MPs into living cells

While the PAMPA method is used routinely to assess passive membrane permeability, it employs an artificial membrane. To obtain a preliminary assessment of the ability of IP+ MPs to enter living cells, we employed the chloroalkane penetration assay (CAPA).{Peraro, 2017 #6544} In this protocol, cells expressing HaloTag protein (HTP) are incubated with a chloroalkane (CA)-tagged molecule of interest (MOI) for a defined period of time. Excess CA-MOI is washed away and the cells are then treated with a CA-coupled fluorescent dye. Finally, excess dye is washed away and the level of fluorescence retained by the cells is assessed by fluorescence cell sorting. This assay is repeated at several different MOI-CA concentrations. The more permeable the MOI-CA conjugate, the less intense the cellular fluorescence will be since the HTP active site is blocked from reacting with the CA-dye conjugate.

The chloroalkane-bearing IP+ macrocycles (**MPs 51-54**) shown in Figure 9 were synthesized, purified, and subjected to the CAPA using HEK293 cells stably expressing HTP. A Lipinski-compliant tryptophan-CA conjugate was used as a control for comparative purposes. These MPs are analogues of **MP35**, **MP36**, **MP37** and **MP40** (Figure 8) but were constructed using Py25 (Figure 2B) to allow attachment of the CA tag to the secondary amine of the piperdine moiety. As shown in Figure 9, the IP+ MP-CA conjugates display CP_{50} values between 0.9 μM and 2.7 μM, whereas the Trp-CA Lipinski-compliant molecule displayed a CP_{50} value of 0.11 μM (see Supplementary Figures 88-93 for the raw data). Thus, the MP-CA conjugates are approximately 8- to 25-fold less cell permeable than the Trp-CA control. We consider this to be a promising result given the much higher molecular masses of the MPs. A much more comprehensive analysis of the cell permeability of these MPs is underway and will be reported in due course.

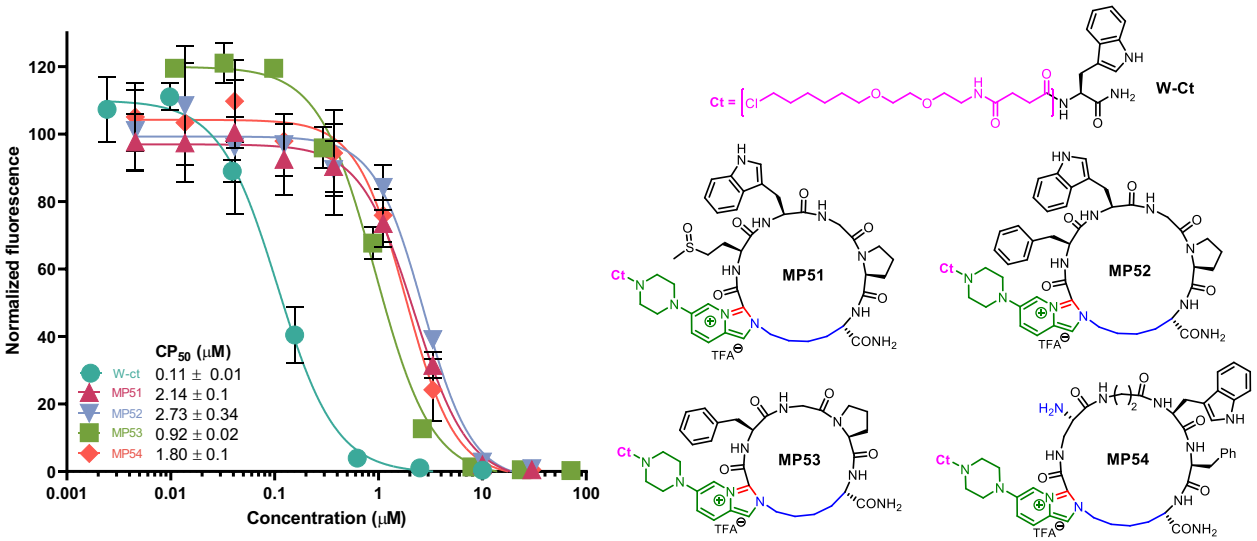

Figure 9. Determination the cell permeability of IP$^+$ MPs. HEK293 cells stably expressing HTP were incubated with the indicated compound for five hours at 37 ºC. After washing, the cells were lysed and the extract was treated with a biotin-CA conjugate to alkylate HTP not already occupied by the MP-CA conjugate. The extracts were then subjected to SDS-PAGE and Western blotting using fluorescently labeled Streptavidin. The amount of fluorescent protein (normalized to total HTP) under the conditions employed are shown on the left. The structures of the compounds employed in this experiment are shown on the right.

Stability of IP+ MPs under physiological conditions

IP$^+$ macrocycles have the potential to act as electrophiles. To determine if typical cellular nucleophiles are reactive with IP$^+$ MPs, **MP12**, **MP14** and **MP16** were incubated with glutathione (5mM) or 2-

mercaptoethanol (5 mM), at 37 °C for 24 hours. LC-MS analysis of the solutions showed that the IP+ MP were stable under these conditions; no new peaks were observed. A similar experiment was done using the amine nucleophiles hydrazine and piperidine with the same result. We conclude that the IP+ MP are stable under physiological conditions with respect to reaction with nucleophiles.

The stability of IP^+ MPs to acid, basic, oxidizing and reducing conditions was evaluated by incubating the macrocycles with 5 mM $NaIO_4$, sodium dithionite ($Na_2S_2O_4$), or triisopropyl silane (TIPS) at 37 °C for 24 hours. Again, no products were observed by LC-MS. Finally, the macrocycles were incubated in in buffers with pH values ranging from 1 to 11. LC-MS analysis showed the macrocycles to be stable under all of these conditions.

The primary data for all of these experiments is shown in Supplementary Figures 94-96.

Discussion

MPs have been shown to be capable of engaging difficult-to-drug proteins with shallow binding pockets but the relatively poor membrane permeability and bioavailability of most MPs have limited their utility in addressing intracellular targets. Therefore, there is a high degree of interest in the discovery of novel MPs with improved pharmacokinetic properties. Several investigators have developed variants of cell-penetrating peptides to solve this problem.[22] These are cationic oligomers that are thought to bind to the plasma membrane and trigger the formation of an endocytotic vesicle.[23] This is very different from achieving passive permeability in that the MP must eventually escape from the endosome. While there has been significant progress in this vein,[24] there is lingering concern about toxicity in employing this mechanism of action to gain entry of MPs into cells.

It is well established that one of the principal barriers to the passive permeation of peptides across membranes is the presence of multiple polar, highly hydrated, N-H amide bonds.[2, 25] Indeed, the unusually high bioavailability of certain peptide-based natural products, such as cyclosporine, can be ascribed to a high degree of N-methylation as well as the ability to adopt conformations that "hide" the remaining N-H units from solvent through intramolecular hydrogen bonding.[2] Thus, many strategies for improving the passive membrane permeability of MPs have focused on mimicking these characteristics. For example, some stapled peptides achieve this goal by stabilizing a helical structure with multiple intramolecular hydrogen bonds. Hydrophobic staples also generally improve permeability.[26] An emerging strategy, nicely represented by a recent report from Suga and colleagues,[27] is to incorporate into the macrocycle non-amino acid units (in this case two pyridine rings) that are positioned to enter into intramolecular hydrogen bonds with N-H units in the peptide chain.

An alternative approach, represented by the present study, is to include in the ring units that improve the passive permeability of the MPs irrespective of the conformation of the peptide. We hypothesized that the permanent positive charge on the IP^+ heterocycle would attract IP^+-containing MPs to a membrane, and that the hydrophobic nature of the ring system would facilitate movement across it. The PAMPA data shown in Figure 8 strongly support this notion. 45% of the IP+-containing MPs analyzed displayed excellent passive permeability ($-\log P_e < 6.0$) despite the fact that their molecular weights ranged from 650-850 Daltons. Even very large macrocycles with molecular weights of > 1000 Daltons (**MP18** and **MP19**) displayed moderate passive permeability (-logPe = 6.4 and 6.3, respectively). This is clearly due to an effect of the IP^+ unit, as demonstrated by a comparison of the membrane permeabilities of comparable peptides cyclized using different linkage strategies (Figure 8, yellow dots). Preliminary CAPA data also show that these IP^+ MPs readily access the cytosol of living cells (Figure 9).

Another interesting point is that the substitution on the IP^+ unit also influences permeability substantially (compare **MP38-MP41** in the second row of Figure 8B). While we cannot rule out the possibility that this influences the conformation of the macrocycle, it seems more likely that this is a direct effect of the

chemical and physical properties of the IP^+ moiety. For example, the hydrophobic, electron-donating piperidine ring in **MP40** appears to promote permeability to a greater degree than fused aromatic rings (**MP38**, **MP39** and **MP41**). It will be interesting in the future to thoroughly assess substitution effects on the permeability of otherwise identical IP^+ MPs.

It is useful to note that all of these molecules contain a C-terminal primary amide unit formed by cleavage of the RAM linker. This is detrimental to cell permeability. Thus, it is likely that even more permeable MPs can be developed by employing different linkage chemistry for the solid-phase synthesis. Likewise, incorporation of N-methylated amino acids would likely lead to improved permeability as well.

Combined with the broad utility of IP^+ formation for the efficient closure of macrocyclic rings of different sizes and compositions, these data suggest that this class of molecules is ideally suited for use in combinatorial library synthesis and screening with a reasonable expectation that the derived ligands against intracellular targets will show activity in living cells and animals.

Associated Content

Supporting Information

Description of methods, supplementary figures and data for compound characterization (PDF).

Author Information

Corresponding Author

Thomas Kodadek – Department of Chemistry, The Herbert Wertheim UF Scripps Institute for Biomedical Innovation and Technology, 120 Scripps Way, Jupiter, FL: 33458. USA. ORCID.org/0000-0003-1930-4795; E-mail: kodadek@ufl.edu.

Authors

Bo Li - Department of Chemistry, The Herbert Wertheim UF Scripps Institute for Biomedical Innovation and Technology, 120 Scripps Way, Jupiter, F: 33458. USA. ORCID,org/0000-0003-2914-9178; E-mail: boli1@ufl.edu

Joshua Parker - Department of Chemistry, The Herbert Wertheim UF Scripps Institute for Biomedical Innovation and Technology, 120 Scripps Way, Jupiter, F: 33458 USA. Skaggs Graduate School of Chemical and Biological Sciences. ORCID.org/0009-0004-0221-1108; E-mail: Joshua.Parker@ufl.edu.

Joel Tong - Department of Chemistry, The Herbert Wertheim UF Scripps Institute for Biomedical Innovation and Technology, 120 Scripps Way, Jupiter, F: 33458 USA. Skaggs Graduate School of Chemical and Biological Sciences. ORCID.org/0000-0002-1506-5777 E-mail: jtongweihao@ufl.edu.

Funding

This research was supported by grants from the National Institutes of Health (R35 GM151875) and the National Cancer Institute (R21 CA273954), and a generous gift from the Klorfine Foundation.

Notes

T.K. is a significant shareholder in Deluge Biotechnologies and Triana Biomedicines.

Acknowledgements

We thank Dr. Madeline Balzarini for providing the HEK293-derived stable cell line expressing HTP.

Literature Cited

(1) (a) Vinogradov, A. A.; Yin, Y.; Suga, H. Macrocyclic Peptides as Drug Candidates: Recent Progress and Remaining Challenges. *Journal of the American Chemical Society* **2019**, *141* (10), 4167-4181. (b) Kingwell, K. Macrocycle drugs serve up new opportunities. *Nature Rev. Drug Disc.* **2023**, *22*, 771-773. (c) Ji, X.; Nielsen, A. L.; Heinis, C. Cyclic Peptides for Drug Development. *Angewandte Chemie International Edition* **2023**, e202308251.

(2) Ahlbach, C. L.; Lexa, K. W.; Bockus, A. T.; Chen, V.; Crews, P.; Jacobson, M. P.; Lokey, R. S. Beyond cyclosporine A: conformation-dependent passive membrane permeabilities of cyclic peptide natural products. *Future Med Chem* **2015**, *7* (16), 2121-2130.

(3) Heinis, C.; Winter, G. Encoded libraries of chemically modified peptides. *Curr Opin Chem Biol* **2015**, *26*, 89-98.

(4) (a) Josephson, K.; Ricardo, A.; Szostak, J. W. mRNA display: from basic principles to macrocycle drug discovery. *Drug Discovery Today* **2014**, *19* (4), 388-399. (b) Goto, Y.; Suga, H. The RaPID Platform for the Discovery of Pseudo-Natural Macrocyclic Peptides. *Accounts of Chemical Research* **2021**, *54* (18), 3604-3617.

(5) (a) Onda, Y.; Bassi, G.; Elsayed, A.; Ulrich, F.; Oehler, S.; Plais, L.; Scheuermann, J.; Neri, D. A DNA-Encoded Chemical Library Based on Peptide Macrocycles. *Chemistry – A European Journal* **2021**, *27* (24), 7160-7167. (b) Silvestri, A. P.; Zhang, Q.; Ping, Y.; Muir, E. W.; Zhao, J.; Chakka, S. K.; Wang, G.; Bray, W. M.; Chen, W.; Fribourgh, J. L.; et al. DNA-Encoded Macrocyclic Peptide Libraries Enable the Discovery of a Neutral MDM2–p53 Inhibitor. *ACS Medicinal Chemistry Letters* **2023**, *14* (6), 820-826.

(6) (a) White, C. J.; Yudin, A. K. Contemporary strategies for peptide macrocyclization. *Nature Chemistry* **2011**, *3* (7), 509-524. (b) Chung, B. K. W.; White, C. J.; Yudin, A. K. Solid-phase synthesis, cyclization, and site-specific functionalization of aziridine-containing tetrapeptides. *Nature Protocols* **2017**, *12* (6), 1277-1287. (c) Frost, J. R.; Scully, C. C. G.; Yudin, A. K. Oxadiazole grafts in peptide macrocycles. *Nature Chemistry* **2016**, *8* (12), 1105-1111. (d) Manicardi, A.; Theppawong, A.; Van Troys, M.; Madder, A. Proximity-Induced Ligation and One-Pot Macrocyclization of 1,4-Diketone-Tagged Peptides Derived from 2,5-Disubstituted Furans upon Release from the Solid Support. *Organic Letters* **2023**, *25* (36), 6618-6622. (e) Lawson, K. V.; Rose, T. E.; Harran, P. G. Template-constrained macrocyclic peptides prepared from native, unprotected precursors. *Proceedings of the National Academy of Sciences* **2013**, *110* (40), E3753. (f) Mendoza, A.; Bernardino, S. J.; Dweck, M. J.; Valencia, I.; Evans, D.; Tian, H.; Lee, W.; Li, Y.; Houk, K. N.; Harran, P. G. Cascade Synthesis of Fluorinated Spiroheterocyclic Scaffolding for Peptidic Macrobicycles. *Journal of the American Chemical Society* **2023**, *145* (29), 15888-15895.

(7) Adebomi, V.; Cohen, R. D.; Wills, R.; Chavers, H. A. H.; Martin, G. E.; Raj, M. CyClick Chemistry for the Synthesis of Cyclic Peptides. *Angewandte Chemie International Edition* **2019**, *58* (52), 19073-190.

(8) (a) Botti, P.; Pallin, T. D.; Tam, J. P. Cyclic Peptides from Linear Unprotected Peptide Precursors through Thiazolidine Formation. *Journal of the American Chemical Society* **1996**, *118* (42), 10018-10024. (b) Bell, H. J.; Malins, L. R. Peptide macrocyclisation via late-stage reductive amination. *Organic & Biomolecular Chemistry* **2022**, *20* (31), 6250-6256. (c) Yamaguchi, A.; Kaldas, S. J.; Appavoo, S. D.; Diaz, D. B.; Yudin, A. K. Conformationally stable peptide macrocycles assembled using the Petasis borono-Mannich reaction. *Chemical Communications* **2019**, *55* (71), 10567-10570. (d) Malins, L. R.; deGruyter, J. N.; Robbins, K. J.; Scola, P. M.; Eastgate, M. D.; Ghadiri, M. R.; Baran, P. S. Peptide

Macrocyclization Inspired by Non-Ribosomal Imine Natural Products. *Journal of the American Chemical Society* **2017**, *139* (14), 5233-5241. (e) Zhang, Y.; Zhang, Q.; Wong, C. T. T.; Li, X. Chemoselective Peptide Cyclization and Bicyclization Directly on Unprotected Peptides. *Journal of the American Chemical Society* **2019**, *141* (31), 12274-12279. (f) Todorovic, M.; Schwab, K. D.; Zeisler, J.; Zhang, C.; Bénard, F.; Perrin, D. M. Fluorescent Isoindole Crosslink (FIICk) Chemistry: A Rapid, User-friendly Stapling Reaction. *Angewandte Chemie International Edition* **2019**, *58* (40), 14120-14124.

(9) Hutt, J. T.; Aron, Z. D. Efficient, Single-Step Access to Imidazo[1,5-a]pyridine N-Heterocyclic Carbene Precursors. *Organic Letters* **2011**, *13* (19), 5256-5259.

(10) (a) Santoro, A.; Lord, R. M.; Loughrey, J. J.; McGowan, P. C.; Halcrow, M. A.; Henwood, A. F.; Thomson, C.; Zysman-Colman, E. One-Pot Synthesis of Highly Emissive Dipyridinium Dihydrohelicenes. *Chemistry – A European Journal* **2015**, *21* (19), 7035-7038. (b) Singh, D.; Sharma, S.; Kumar, M.; Kaur, I.; Shankar, R.; Pandey, S. K.; Singh, V. An AcOH-mediated metal free approach towards the synthesis of bis-carbolines and imidazopyridoindole derivatives and assessment of their photophysical properties. *Organic & Biomolecular Chemistry* **2019**, *17* (4), 835-844. (c) Buvaylo, E. A.; Kokozay, V. N.; Linnik, R. P.; Vassilyeva, O. Y.; Skelton, B. W. Hybrid organic–inorganic chlorozincate and a molecular zinc complex involving the in situ formed imidazo[1,5-a]pyridinium cation: serendipitous oxidative cyclization, structures and photophysical properties. *Dalton Transactions* **2015**, *44* (30), 13735-13744. (d) Li, X.; Zhang, K.; Wang, G.; Yuan, Y.; Zhan, G.; Ghosh, T.; Wong, W. P. D.; Chen, F.; Xu, H.-S.; Mirsaidov, U.; et al. Constructing ambivalent imidazopyridinium-linked covalent organic frameworks. *Nature Synthesis* **2022**, *1* (5), 382-392.

(11) Lipinski, C. A.; Lombardo, F.; Dominy, B. W.; Feeney, P. J. Experimental and computational approaches to estimate solubility and permeability in drug discovery and developmental settings. *Adv. Drug Deliv. Rev.* **1997**, *23*, 3-25.

(12) Bosch, P.; García, V.; Bilen, B. S.; Sucunza, D.; Domingo, A.; Mendicuti, F.; Vaquero, J. J. Imidazopyridinium cations: A new family of azonia aromatic heterocycles with applications as DNA intercalators. *Dyes and Pigments* **2017**, *138*, 135-146.

(13) Patnaik, S.; Marugan, J. J.; Liu, K.; Zheng, W.; Southall, N.; Dehdashti, S. J.; Thorsell, A.; Heilig, M.; Bell, L.; Zook, M.; et al. Structure–Activity Relationship of Imidazopyridinium Analogues as Antagonists of Neuropeptide S Receptor. *Journal of Medicinal Chemistry* **2013**, *56* (22), 9045-9056.

(14) Kaminski, J. J.; Doweyko, A. M. Antiulcer Agents. 6. Analysis of the in Vitro Biochemical and in Vivo Gastric Antisecretory Activity of Substituted Imidazo[1,2-a]pyridines and Related Analogues Using Comparative Molecular Field Analysis and Hypothetical Active Site Lattice Methodologies. *Journal of Medicinal Chemistry* **1997**, *40* (4), 427-436.

(15) Khatun, S.; Singh, A.; Bader, G. N.; Sofi, F. A. Imidazopyridine, a promising scaffold with potential medicinal applications and structural activity relationship (SAR): recent advances. *J Biomol Struct Dyn* **2022**, *40* (24), 14279-14302.

(16) Geoghegan, K. F.; Stroh, J. G. Site-directed conjugation of nonpeptide groups to peptides and proteins via periodate oxidation of a 2-amino alcohol. Application to modification at N-terminal serine. *Bioconjugate Chemistry* **1992**, *3* (2), 138-146.

(17) Yamasaki, R. B.; Osuga, D. T.; Feeney, R. E. Periodate oxidation of methionine in proteins. *Analytical Biochemistry* **1982**, *126* (1), 183-189.

(18) (a) Walensky, L. D.; Kung, A. L.; Escher, I.; Malia, T. J.; Barbuto, S.; Wright, R. D.; Wagner, G.; Verdine, G. L.; Korsmeyer, S. J. Activation of apoptosis in vivo by a hydrocarbon-stapled BH3 helix. *Science* **2004**, *305* (5689), 1466-1470. (b) Walensky, L. D.; Bird, G. H. Hydrocarbon-stapled peptides: principles, practice, and progress. *J Med Chem* **2014**, *57* (15), 6275-6288.

(19) Zhang, H.; Zhao, Q.; Bhattacharya, S.; Waheed, A. A.; Tong, X.; Hong, A.; Heck, S.; Curreli, F.; Goger, M.; Cowburn, D.; et al. A Cell-penetrating Helical Peptide as a Potential HIV-1 Inhibitor. *Journal of Molecular Biology* **2008**, *378* (3), 565-580.

(20) Alluri, P. G.; Reddy, M. M.; Bachhawat-Sikder, K.; Olivos, H. J.; Kodadek, T. Isolation of protein ligands from large peptoid libraries. *J Am Chem Soc* **2003**, *125* (46), 13995-14004.

(21) MacConnell, A. B.; McEnaney, P. J.; Cavett, V. J.; Paegel, B. M. DNA-Encoded Solid-Phase Synthesis: Encoding Language Design and Complex Oligomer Library Synthesis. *ACS Comb Sci* **2015**, *17*, 518-534.

(22) Koren, E.; Torchilin, V. P. Cell-penetrating peptides: breaking through to the other side. *Trends in Molecular Medicine* **2012**, *18* (7), 385-393. Wender, P. A.; Mitchell, D. J.; Pattabiraman, K.; Pelkey, E. T.; Steinman, L.; Rothbard, J. B. The Design, Synthesis, and Evaluation of Molecules That Enable or Enhance Cellular Uptake: Peptoid Molecular Transporters. *Proc. Natl. Acad. Sci. USA* **2000**, *97*, 13003-13008.

(23) Doherty, G. J.; McMahon, H. T. Mechanisms of Endocytosis. *Annual Review of Biochemistry* **2009**, *78* (1), 857-902.

(24) (a) Lian, W.; Jiang, B.; Qian, Z.; Pei, D. Cell-Permeable Bicyclic Peptide Inhibitors against Intracellular Proteins. *Journal of the American Chemical Society* **2014**, *136* (28), 9830-9833. (b) Qian, Z.; Martyna, A.; Hard, R. L.; Wang, J.; Appiah-Kubi, G.; Coss, C.; Phelps, M. A.; Rossman, J. S.; Pei, D. Discovery and Mechanism of Highly Efficient Cyclic Cell-Penetrating Peptides. *Biochemistry* **2016**, *55* (18), 2601-2612.

(25) Yu, P.; Liu, B.; Kodadek, T. A high-throughput assay for assessing the cell permeability of combinatorial libraries. *Nat Biotechnol* **2005**, *23* (6), 746-751.

(26) Chu, Q.; Moellering, R. E.; Hilinski, G. J.; Kim, Y.-W.; Grossmann, T. N.; Yeh, J. T. H.; Verdine, G. L. Towards understanding cell penetration by stapled peptides. *MedChemComm* **2015**, *6* (1), 111-119.

(27) Chen, H.; Katoh, T.; Suga, H. Macrocyclic Peptides Closed by a Thioether-Bipyridyl Unit That Grants Cell Membrane Permeability. *ACS Bio Med Chem Au* **2023**, *3* (5), 429-437.

518 Table of Contents Graphic

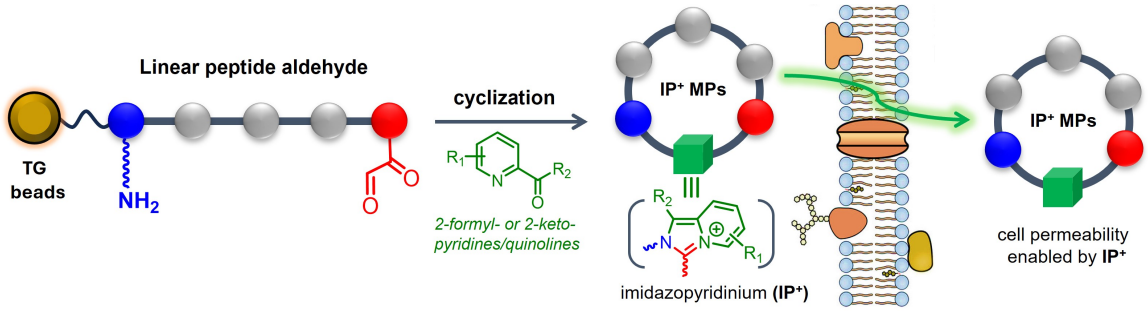

519

520